Automation in Construction 110 (2020) 103007

Contents lists available at ScienceDirect

Automation in Construction

journal homepage: www.elsevier.com/locate/autcon

# Combined fuel consumption and emission optimization model for heavy construction equipment

Masoud Masih-Tehrani*, Salman Ebrahimi-Nejad, Masoud Dahmardeh

*Vehicle Dynamical System Research Lab, School of Automotive Engineering, Iran University of Science and Technology, Tehran, Iran*

ARTICLE INFO

*Keywords:*
Bulldozer
Building and construction
Environmental impacts
Digging optimization
Fuel consumption
Emission reduction

ABSTRACT

In this paper, a novel optimization model is developed for heavy construction equipment. This approach investigates a complete range of engine operating points, considering fuel consumption and emission maps to accurately model fuel efficiency and level of emissions in different working conditions. As a case study, a tracked bulldozer is investigated on different terrains. The target of the optimization problem is defined as a specific digging or grading depth with minimum fuel consumption and emissions (unburned hydrocarbons, carbon monoxide, and nitrogen oxides) based on EU non-road diesel engine emission standard values. Interaction between the terrain and the bulldozer track is modeled using a semi-empirical method. Dry sand, clayey soil, and snow terrain are considered. The studied bulldozer is a Caterpillar D8T with 233 kW engine power and 8A type blade. The design variables are engine speed, transmission gear number, and throttle position. Genetic algorithm, a famous optimization method, is employed. In order to reduce computational costs, integer programming genetic algorithm is utilized. Due to the complexity of the problem, a constrained nonlinear optimization problem with combined-objectives is developed. Results show that the general trend of fuel consumption and emissions rise as the digging depth increases, as expected. However, this study indicates that the bulldozer traction and digging control can be effectively manipulated by controlling the engine operating point, characterized by engine speed and gear number, to obtain significant improvements in fuel consumption and reduction of exhaust emissions. The results also indicate that re-performing the optimizing problem for different terrain types leads to optimized fuel and emissions targets of up to 77%.

## 1. Introduction

Environmental aspects of transportation have attracted the attention of researchers and regulators globally in order to develop energy-efficient technologies and devise policies aimed at the reduction of adverse environmental effects [1, 2]. Although the building and construction sector is one of the seven dominant sectors that significantly contribute toward global greenhouse gas emissions [3, 4], however, the industry is mainly directed toward energy optimization in buildings and the sustainability of construction materials to use resources more efficiently [5-7]. Therefore, the environmental impacts of heavy construction vehicles (such as bulldozers, dumper trucks, and excavators) are used to be neglected in most air pollution studies [8]. However, heavy off-the-road machinery is in constant use for building and construction works and infrastructure engineering projects, with annual worldwide sales of 0.6-1 million units [8]. Moreover, recent reports studying life cycle environmental effects of a building during construction, maintenance, demolition, and recycling phases, have paid particular attention to heavy construction vehicles and heavy-duty transport [9-11].

A “bulldozer” consists of a tractor (usually a tracked one) equipped with a blade. Generally, it is used to push large amounts of soil, sand, rubble, etc. during construction or conversion work. Bulldozers are employed on a wide range of building, construction, and mining sites, massive industry factories, engineering projects, and farms [12, 13]. Determination of the tracked vehicles traction force has been a popular field of study in terramechanics [14, 15]. Various bulldozer modeling studies are reported. Multi-body dynamics are used to model various bulldozer components, as well as the associated joints and contact surfaces [16]. High fidelity multi-body dynamics analysis can be used to optimize the design of bulldozers and their subsystems. San [17] employed finite element method to model a bulldozer multi-body dynamics, although, at high computational costs.

The remainder of the manuscript is organized as follows. First, a review of the background is presented in Section 2, and the problem statement of the research is described. Then, we present the research

* Corresponding author.
*E-mail addresses:* masih@iust.ac.ir (M. Masih-Tehrani), ebrahiminejad@iust.ac.ir (S. Ebrahimi-Nejad), mdahmardeh@iust.ac.ir (M. Dahmardeh).

https://doi.org/10.1016/j.autcon.2019.103007
Received 10 November 2018; Received in revised form 6 October 2019; Accepted 2 November 2019
0926-5805/ © 2019 Elsevier B.V. All rights reserved.

methodology in Section 3. In Section 3.1, the Caterpillar D8T bulldozer is introduced, and the powertrain is modeled, in order to analyze fuel consumption and emission behavior. The complex multi-body dynamics employed for modeling of the bulldozer [17] are simplified using semi-empirical models of the vehicle-terrain interaction. The engine model which takes into account fuel consumption rate and emission behavior (*HC*, *CO*, and *NOx*) are introduced in Section 3.1. The vehicle-terrain interaction is modeled using a semi-empirical method proposed by Bekker [18] in Section 3.2. InSection 3.3, the bulldozer minimum fuel consumption and emissions program is developed. Finally, the obtained results are discussed in Section 4, and concluding remarks are presented in Section 5.

## 2. Background and problem statement

Various researchers present analyses of electric and hybrid bulldozers. Zhang et al. [19] proposed a model using the subsequent development of ADvanced VehIcle SimulatOR (ADVISOR). The model is employed to analyze the performance during straight movement and steering conditions. Bulldozer's dynamics model, track walking mechanism model, oil pump model, etc. are also developed employing MATLAB/Simulink. Pan et al. [20] studied the electric drive system of a tracked hybrid bulldozer. A multi-energy management strategy is employed, and a method for minimizing the fuel consumption and emission of a hybrid bulldozer is presented. Wang et al. [21] investigated the fuel economy of a series hybrid electric tracked bulldozer (HETB) through the developed model. A model predictive controller (MPC) as the energy management system is reported.

Lewis and Hajji [22, 23] developed a productivity rate model for a piece of construction equipment. The productivity rate is defined as the ratio of the quantity of the work completed to the duration of the process. Therefore, the productivity rate is inversely related to the duration of the process. Thus, it is necessary to predict the productivity rates of construction equipment in order to estimate emissions. Hajji [24] proposed a model to estimate $CO_2$ emission concerning to the productivity rate. However, other emissions such as un-burned hydrocarbons *HC*, carbon monoxide *CO*, and nitrogen oxide *NOx* are not considered. These emissions are reported by other groups [25, 26]. In these reports, the amount of emission is quantified through *the emission factor* and *load factor*. The former models the level of emission, while the later models the average employed rated power used, considering operation at idle, partial loads, etc. The US Environmental Protection Agency (EPA) developed the NONROAD model, considering engine load, fuel-to-emission ratio, and engine size [27]. These studies investigate specific operating points and usually lack accurate modeling of the construction equipment (engine), as well as emission maps which accurately model the level of emission at different engine operating points and working conditions.

Multi-objective optimization of vehicle traction is proposed by Robinson et al. [28] for a wheeled vehicle driving in loose dry sand. The maximum slope climbing efficiency is defined as the primary objective function during the optimization process. Design variables are ground and traction parameters such as drawbar pull (DBP), motion resistance (MR), longitudinal traction coefficient (LTC), and lateral force coefficient (LFC). The proposed optimization problem has eight design constraints: limitation of tire deflections and corresponding DBP coefficients. The generalized reduced gradient method is employed to find optimal values of the design variables. The model is based on the Vehicle Terrain Interface (VTI) model proposed by Vahedifard et al. in Ref. [29]. However, fuel consumption and emissions are not considered in these studies.

Due to the ever-increasing significance of heavy construction vehicles, in the context of environmental impacts of building and construction projects, in this article, the bulldozer digging (soil pushing) program is considered, and an optimization problem is developed to minimize fuel consumption and emission (considering *HC*, *CO*, and *NOx*). This manuscript focuses on the development of a novel optimization approach, able to investigate a complete range of construction equipment engine operating points, and accurately select the working conditions leading to a minimized function of emission level and fuel efficiency. As pointed out, those emission items are introduced as the cost function into the optimization problem. In this case, as $CO_2$ is closely related to fuel consumption [30-32], only the latter is considered in order to simplify the problem. Also, throughout the paper, the “digging depth” is interpreted as the height of the soil accumulated within the bucket. It should be noted that since the studied terrains are not limited to soil; therefore, “soil height” or similar phrases are not used. The optimization design variables are engine speed, engine throttle position, and transmission gear number. The genetic algorithm (GA), a popular optimization method [33], is employed to solve the proposed non-linear constrained problem.

The primary pollutants i.e., hydrocarbon *HC*, carbon monoxide *CO*, and nitrogen oxide *NOx*, are considered to evaluate the level of emission during the optimization process [34]. Hydrocarbon emission, which is formed due to the incomplete combustion of fuel, as well as fuel evaporation, is toxic and causes short-term or long-term effects, such as cancer. Carbon monoxide is a colorless, odorless and tasteless gas which is formed by incomplete combustion of any hydrocarbon gas. It reacts with human blood hemoglobin and prevents oxygen transfer. High levels of it cause vision problems and even death. Nitrogen oxide contributes to the formation of smog, as well as acid deposition. It damages plants and animals, and ultimately damaging human health. The reaction between nitrogen oxide and volatile organic compounds can lead to the formation of ozone which causes severe damage to the eyes, nose, and respiratory system. It also causes damage to plants, crops, and forests [35].

In order to show the reliability of the proposed approach, a case study is presented, including a tracked bulldozer on different terrains, for which the target of the optimization problem is defined as the digging depth which results in minimized fuel consumption and emissions. Different terrains, including dry sand, clayey soil, and snow, are also considered to generalize the method further and show its effectiveness and potentials in solving problems with various input parameters. Furthermore, other case studies of the optimization algorithm may be developed using vehicles with different transmission characteristics and engine curves, the results of which can also lead to the determination of optimal working point. Finally, the presented optimization approach applies to other heavy construction equipment using different optimization targets to exploit the optimal working condition for minimized fuel consumption and emissions. Future experimental studies may be conducted on machinery in a variety of different test conditions to prove the reliability of the proposed procedure in practice further.

In this paper, a new strategy is proposed for improving fuel consumption and emissions of a construction vehicle (bulldozer is investigated as a case study). In the next stages of future research works, the modeling may incorporate soil type identification process, as well as an observer for the blade or bucket load. Combining these features, the optimum digging program can be employed in practice; the vehicle identifies the soil type and based on the digging load estimation, the optimal working program (e.g., gear number, engine rpm, and throttle position) is selected, which is pre-instructed to the vehicle controller ROM by an offline optimization process. Therefore, the minimum fuel consumption and emissions during an excavating round are achieved. As a custom, the overall work and productivity are the concerns in excavation contracts. The novel approach of this manuscript is focused on the aspects of terramechanics in order to determine the effect of other conditions, such as soil type, track (wheel) geometry, and blade situations. Moreover, it should be noted that throughout this study, we employed a fixed value for the digging depth, which is good merit for comparison between different cases. Also, it can be generalized to any units of work, for instance, by calculating the volume of the moved soil,

**Table 1**
Main specifications of the Caterpillar D8T bulldozer [36].

| Suspension type | Tracked |
|---|---|
| Track width (m) | 0.610 |
| Track length (m) | 3.206 |
| Operating mass (kg) | 39420 |
| Blade type | 8A |
| Blade width (m) | 5.045 |
| Blade height (m) | 1.177 |
| Maximum digging depth (mm) | 625 |
| Transmission efficiency (%) | 85 |
| Gear 1 (km/h) | 3.4 |
| Gear 2 (km/h) | 6.1 |
| Gear 3 (km/h) | 10.6 |
| Engine power (kW) | 233 |

operation time, costs, etc.

## 3. Methodology

### 3.1. Vehicle modeling

The Caterpillar D8T bulldozer is studied in this paper. The main specifications of the bulldozer are listed in Table 1. Bulldozer D8T is commonly used in mining applications, and can be used to conduct future experimental studies; therefore, this type is chosen over other types of construction machinery, to enable future practical applications.

Experimental specifications for the 3126E Caterpillar engine (275 hp/205 kW) are available through the ADVISOR software provided by the National Renewable Energy Laboratory (NREL), U.S. Department of Energy [37]. The maps for the Caterpillar D8T bulldozer are scaled to be under the rated engine power. The scaling process employed in this manuscript is a standard method reported in the literature [38, 39].

Fig. 1 shows the maps for fuel consumption and emissions of the Caterpillar D8T. The maps are calculated using ADVISOR's data and the scaling process. It should be noted that the provided emission/consumption values are only indicative of an order of magnitude, which essentially means that the comparison among dozer implementation solutions is not always possible. The thick solid lines represent the maximum engine torque envelope. Considering the engine brake specific fuel consumption (BSFC) map, the high efficiency zones are in the median rpm's, when the engine torque is above 800 N· m. In order for the engine to operate in the optimal zone, it is preferred to obtain optimum values for the bulldozer design variables during the optimization process within this zone. Using the quasi-static engine map is a standard method in the literature, and many research works are concentrated on the validation of this approach [40-42].

The engine-out *HC*, *CO*, and *NOx* emission maps are shown in Figs. 1. Employment of normalized values has two advantageous: first, the standard limits which are defined as constraints during the optimization process are stated in the normalized form; second, it is easy to identify the most efficient zones in each contour plot. As construction vehicles are equipped with diesel particulate filters (DPF) to remove soot and other particulate matter (PM) from exhaust gases, PM is not considered as an emission item in this study. As can be seen, low emission zones are quite different for the three types of emissions, and these patterns also differ from the fuel efficiency map. Therefore, the optimization process results are non-dominant ones. In other words, improving one objective function may deteriorate other objective functions from their optimum values. Therefore, a trade-off between the objective functions, i.e., fuel consumption and engine emissions exist. Choosing an appropriate optimization technique to solve the proposed nonlinear problem is essential.

### 3.2. Vehicle-terrain interaction modeling

In order to study the effect of terrain type on the traction optimization problem, three different terrain types are studied. The optimization formulation is defined in the next section. Table 2 lists the terrain specifications used for the optimization process. The uncertainty ranges (i.e., confidence intervals) for the terrain specifications (e.g., in terms of mean + / −STD or shaded area) are used by some research works [26, 43]. In this paper, due to the employment of experimental data from other references, the uncertainty ranges are not considered.

A semi-empirical method is proposed by Bekker [45] to investigate motion resistance and traction force of a tracked vehicle. The method proposed by Bekker assumes that the track has a rigid footing and the vertical force applied by the terrain to the track is equivalent to the one beneath a sinkage plate at the same depth in the pressure-sinkage test. If the longitudinal position of the center of gravity for the vehicle is located at the center of the track contact length, the normal pressure distribution is assumed to be uniform. The Bekker's pressure-sinkage equation describes the track sinkage $z_0$ by [46]:

$$z_0 = \left(\frac{p}{k_c/b + k_\phi}\right)^{1/n} = \left(\frac{W/bl}{k_c/b + k_\phi}\right)^{1/n} \tag{1}$$

where $p$ is the normal pressure, $W$ is the normal load applied to the track, $b$ is the width of the track, and $l$ is the track length. Parameters $k_\phi$, $k_c$, and $n$ are given in Table 2. The motion resistance ($R_c$) due to the pressing of the terrain by a track with uniform pressure distribution is expressed by:

$$R_c = \frac{1}{(n+1)b^{1/n}(k_c/b + k_\phi)^{1/n}}\left(\frac{W}{l}\right)^{(n+1)/n} \tag{2}$$

And the drawbar pull ($F_{DP}$) is related to the vehicle thrust, $F$, as:

$$F_{DP} = F - R_c \tag{3}$$

For a regular track with constant normal pressure, the drawbar pull-slip relation is expressed as:

$$\begin{aligned} F_{DP} &= b\int_0^l \left(c + \frac{W}{bl}\tan\phi\right)(1 - \mathrm{e}^{-ix/K})dx \\ &= (Ac + W\tan\phi)\left[1 - \frac{K}{il}(1 - \mathrm{e}^{-ix/K})\right] \end{aligned} \tag{4}$$

where $i$ is the track slip (decimal), $x$ is the longitudinal direction, $K$ is the shear deformation modulus, and $A$ is the track area. The cohesion ($c$) and angle of shearing resistance ($\phi$) are listed in Table 2, and the drawbar pull-slip curve for the dry sand is plotted in Fig. 2.

In order to carry out sensitivity analysis, all of the parameters affecting the drawbar pull are increased and decreased by 10%, and the resultant forces are plotted in Fig. 3. These curves show that a 10% deviation in the whole parameters of the soil causes a maximum shift by 11% in the drawbar pull.

To investigate the effect of each parameter, the values of the angle of shearing resistance ($\phi$), cohesion ($c$), shear deformation modulus ($K$), and vehicle weight ($W$) are increased and decreased independently by 10% at a specific slip value (20%) and the resultant thrust forces are plotted in Fig. 4. The results indicate that two-parameters, i.e. the angle of shearing resistance and vehicle weight have more effect on the resultant drawbar pull, compared with the other parameters. Moreover,

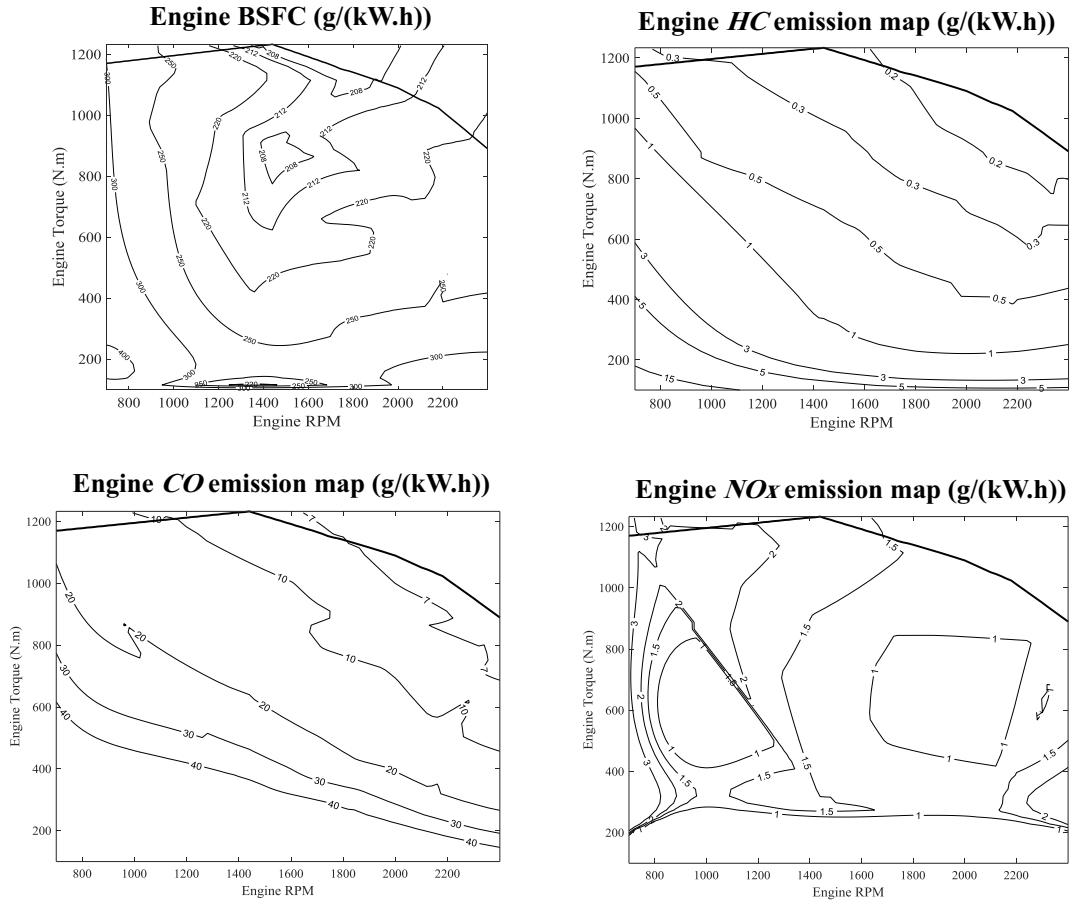


**Fig. 1.** Engine maps of brake specific fuel consumption and engine-out emissions of HC, CO, and NOx.

**Table 2**
Terrain specifications [44].

| Parameter | Description | Unit | Dry sand |
|---|---|---|---|
| $n$ | Exponent of sinkage | – | 1.1 |
| $\phi$ | Angle of shearing resistance | (Degrees) | 28 |
| $c$ | Cohesion | (kPa) | 1.04 |
| $k_\phi$ | Friction modulus | (kN/m$^{n+2}$) | 1528.43 |
| $k_c$ | Cohesive modulus | (kN/m$^{n+1}$) | 0.99 |

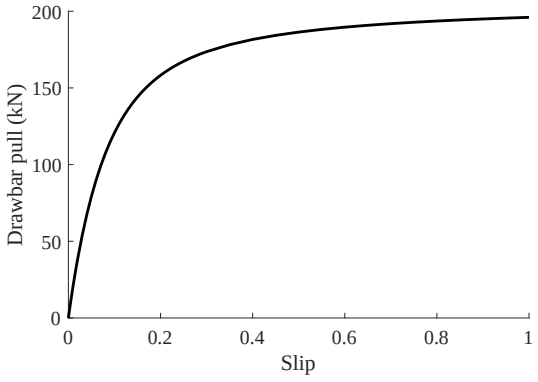


**Fig. 2.** Drawbar pull-slip curves for a tracked vehicle in dry sand.

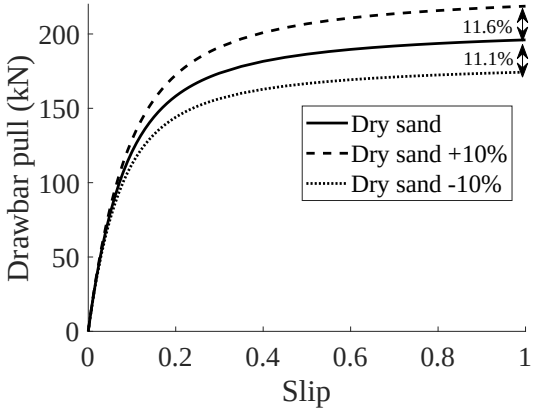


**Fig. 3.** Sensitivity analysis of drawbar pull-slip curves on dry sand.

as the shear deformation modulus increases, the thrust force decreases, which is in contrary to the effects of other parameters.

According to Eqs. (2) to (4), the drawbar pull is dependent on the specifications of the terrain ($n$, $c$, $\phi$, $k_c$, $k_\phi$, $K$), and the vehicle ($W$, $b$, $l$). Moreover, the drawbar pull depends on the track slip ($i$), which in turn is a function of engine operating point. Therefore, the bulldozer traction and digging control can be realized by controlling the engine working point, which is characterized by the engine speed (rpm) and torque (throttle position). As a simple relationship between the accelerator pedal angle and the throttle valve angle (position) exists [47], the throttle position is considered as the control parameter in this study.

The force acting on a vertical bulldozer blade ($F_P$) with a planar surface is normal to the direction of forwarding travel, is given as [44]:

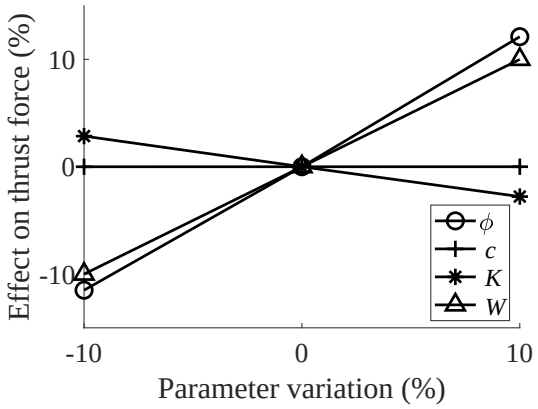


**Fig. 4.** Sensitivity analysis of thrust force at 20% slip on dry sand.

$$F_P = bb\int_0^{h_b}\sigma_p dz = bb\int_0^{h_b}(\gamma_s z N_\phi + 2c\sqrt{N_\phi})dz = bb\left(\frac{1}{2}\gamma_s h_b^2 N_\phi + 2ch_b\sqrt{N_\phi}\right) \quad (5)$$

were $h_b$ is the cutting depth of the blade, $bb$ is the width of the bulldozer blade, $\sigma_p$ is the passive earth pressure, $\gamma_s$ is the weight density of the terrain, and $N_\phi$ is the value of the flow which is given by $\tan^2(45^o + \phi/2)$. An average value for the working conditions and blade load is assumed in order to estimate the drawbar pull with reasonable accuracy in a quasi-static regime.

The relationship between vehicle speed ($V$) and engine speed ($n_e$) is described as:

$$V = \frac{n_e r}{\xi_0}(1 - i) \quad (6)$$

where $r$ is the drive sprocket radius and $\xi_0$ is the total transmission ratio, which is the number of revolutions of the engine crankshaft per revolution of the track drive sprocket. As shown by Eq. (6), the vehicle speed is a function of engine speed and track slip. The track slip is a function of drawbar pull, terrain characteristics, and engine torque.

### 3.3. Fuel consumption and emission optimization

An overview of the optimization problem is shown in Fig. 5. If the digging depth of the bulldozer is specified ($h_{demand}$), the engine is instructed to operate at a specific point in which the fuel consumption and emissions are minimized.

The most relevant variables that control fuel consumption and emissions are provided in the flowchart. However, future sensitivity assessment studies might be conducted to identify the most determinant variables and to evaluate the significance of theoretical uncertainties on the obtained results.

The calculation steps are as follows:

- The gross thrust force is determined using engine torque and total transmission ratio ($\xi_0$).
  The engine torque ($M_e$) is assumed as a nonlinear function of the throttle position ($th$) and engine speed ($n_e$) ([48], Section 2.6) and is expressed by Eq. (7), where the transmission system parameters are not considered.
  $$M_e = M_e(th, n_e) \quad (7)$$
  Throttle position is normalized (between 0% and 100%), where the maximum engine torque at a specific engine speed, $M_{\max}$, is achieved when the throttle is fully opened ($th = 100\%$) (Fig. 6).
  Finally, the thrust force ($F$) is calculated using:
  $$F = \frac{M_e \xi_0 \eta_t}{r} \quad (8)$$
  where $\eta_t$ is the transmission efficiency, a specification of the bulldozer reported in Table 1.
- The track slip ($i$) is determined using the drawbar pull from Fig. 2. In order to calculate the drawbar pull ($F_{DP}$) Eqs. (2), (3), and (8) are used. Both engine rpm and torque dictates the engine operating point. These are transferred to the bulldozer track, which is engaged with the terrain. The tractive force of the vehicle which is generated by the engine is specified by the track slip ($i$), using Eq. (4) in an iterative process. For example, when the engine tries to generate more tractive force (throttle position increases), the track slip increases as well to provide the excess force.
- The digging depth ($h_b$) is calculated by an iterative method from the drawbar pull (Eq. (5)). This variable is utilized as a constraint for the optimization problem.
- The vehicle speed is calculated using Eq. (6).
- In order to solve the proposed optimization problem, genetic algorithm (GA) using MATLAB is employed [49]. The GA method is run for a reasonable time to ensure the convergence to the solution. In each iteration of the GA, the calculated solutions are set as the initial population for the next iteration. Integer programming is selected to reduce the computational cost while maintaining a reasonable accuracy [50].

### 3.4. Weighting factors and constraints

The normalization coefficients employed within the target of the optimization process are calculated using EU non-road diesel engine emission standard limits. The EU non-road diesel engines, Stage II Cat. E (2002) standard [51] sets the limitation for the *HC*, *CO*, and *NOx* pollutants by 1.0, 3.5, and 6.0 g/kWh, respectively. Although EU emission values reflect the achievements in vehicle emission reduction technologies and possible regulatory priorities in different emission items, however, the proposed formulation makes it possible for researchers to focus on any of the emission factors based on the type of application and their respective prioritizing.

The European emission standard for non-road diesel engines is employed here for normalization purposes. The normalization coefficients of fuel consumption and emissions for the optimization problem are listed in Table 3, which are under the standard limitations values provided by the standard.

An iterative process is proposed to find the proper weighting factors assigned to each of the fuel consumption and emission items to be employed for the optimization formulation, and is a common approach reported by many research works [52-54]. Corresponding values are assigned to the weighting factors in the first iteration, and the resultant fuel consumption and emission items are compared to the regulation values. In the next iteration, the weighting factors associated with the target consumption and emission items which are not within the acceptable range of the non-road standard are updated, until satisfactory results are obtained.

As an example, four sets of weighting factors are considered in this study, as shown in Table 3. The first set of weighting factors are considered to have the same value ($\frac{1}{4} = 0.25$ each, with the total weighting factors summation of 1). In order to evaluate the effects of these weighting factors, the optimization process is performed to study the bulldozer performance at a given depth of $h_b = 0.3$ m (as a mean depth value, between 0.1 m to 0.6 m). The obtained results for the first set of weighting factors (Table 3) indicate that although the *NOx* quantity (37.72 g/kWh) is not acceptable within the framework of the EU emission standard for non-road diesel engines (6 g/kWh), however, the *CO* and *HC* values (1.34 and 0.88 g/kWh) are within the acceptable range (3.5 and 1.0 g/kWh). Therefore, in the next step, the second set of weighting factors is defined in order to moderate the high emission

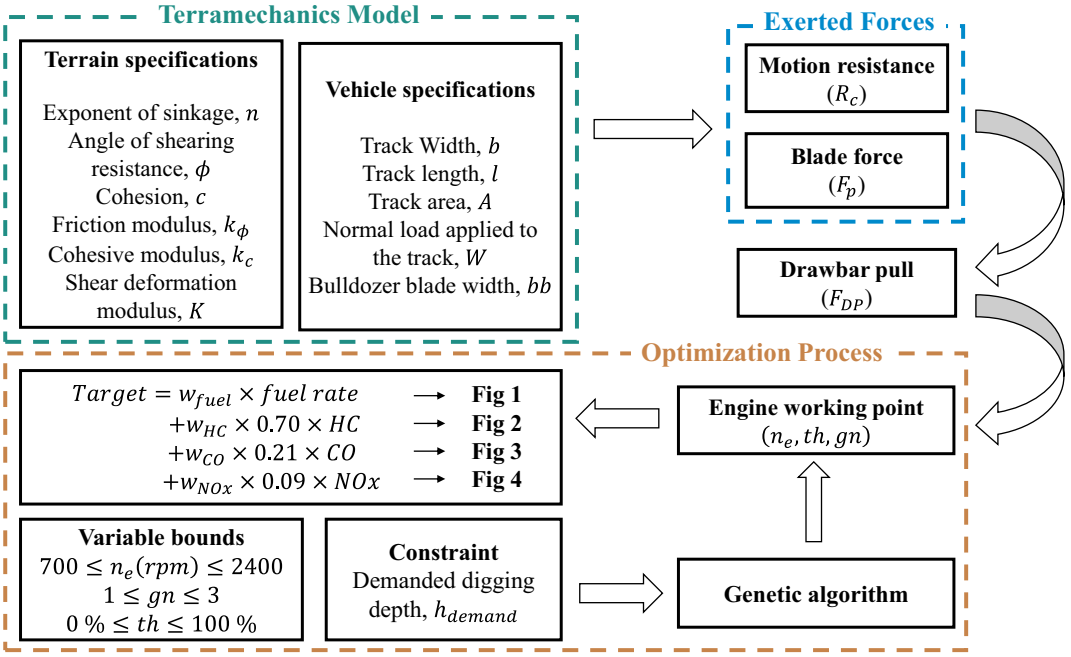


**Fig. 5.** Flowchart of the optimization problem.

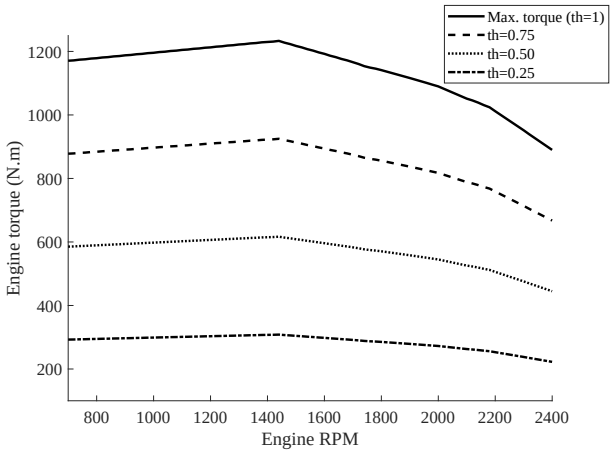


**Fig. 6.** Engine torque in different throttle position and RPM.

levels of *NOx*. Considering Iteration 2, the weighting factors for *fuelrate*, *HC*, and *CO* are decreased compared with the previous iteration, while the *NOx* weighting factor is increased to almost six times of the weighting factor for *fuelrate*, *HC*, and *CO*. The optimization process is repeated for the same excavation depth, and the obtained results indicate that the *NOx* value is improved, however, it is still higher than the standard requirements. Therefore, the third set of weighting factors is studied to compensate for the high levels of the bulldozer *NOx* emissions. The results indicated that the *NOx* value is further improved, yet still higher than the standard requirements. At the fourth step, the *NOx* weighting factor is increased again. As can be seen, the bulldozer performance is the same as that for Iteration 3, since the engine is operating at its best operating point and cannot be further improved. Further reduction of *NOx* emission levels to comply with the standard value may be obtained using exhaust gas after-treatment, including innovative designs of Diesel Particle Filters (DPF's).

As a basic rule, the preliminary optimization aims to follow regulatory limits devised on emission items. Therefore, this procedure is followed in the first iteration to obtain optimized *HC*, *CO*, and *NOx* emission values. However, as *HC* and *CO* values are well below the defined values, the main problem becomes the minimization of NOx emissions, by slightly raising fuel consumption and *CO* emissions, while keeping *HC* and *CO* emissions well below the acceptable EU regulation limits. As the adverse effects of the increase in *CO* emissions or fuel consumption rates are not the main subject of this research, as far as it remains less than the limit, this point is only mentioned in the text, and some discussions are made. However, interested readers are referred to relevant previous research [55] for detailed discussions on this topic and the correlation between *CO* emission and an increase in PM values.

It should be noted that the weighting factors are not direct indicators of the relative importance of individual pollutants, based on the degree of threat posing to public health, environment, etc. The weighting factors are used to indicate the level of emphasis given to each polluting item for achieving the assigned objective standard criteria (which may inherently address public health concerns and priorities).

Therefore, the third set of weighting factors is adopted throughout this article (Table 3, Iteration 3). The procedure described above for selecting the weighting factors is carried out at a digging depth of 0.3 m in dry sand; however, it is almost the same for other cases. The combined optimization problem for simultaneous minimization of fuel consumption and emissions is presented by Eq. (9):

$$\begin{aligned} \text{Minimize: } & Target = 0.03 \times 1.0 \times fuel\ rate(n_e, th, gn) \\ & + 0.03 \times 0.69 \times HC(n_e, th, gn) + 0.03 \times 0.20 \times CO(n_e, th, gn) \\ & + 0.91 \times 0.11 \times NOx(n_e, th, gn) \\ \text{subject to: } & h_b = h_{demand} \end{aligned} \tag{9}$$

As indicated above, the constraint of the proposed optimization problem is digging depth. The optimization parameters are summarized in Table 4. As listed, three design variables with the corresponding bounds are considered.

## 4. Results and discussion

### 4.1. Optimization solutions

Solutions of the proposed optimization problem for minimizing fuel consumption and emissions on dry sand are listed in Table 5.

The objective function of fuel consumption and emissions

**Table 3**
Different sets of weighting factors for fuel consumption and emissions and the corresponding bulldozer performances (at $h_b = 0.3$ m), along with the European emission standards for non-road diesel engines.

| | | Fuel rate | *HC* | *CO* | *NOx* |
|---|---|---|---|---|---|
| EU non-road diesel engines, Stage II Cat. E (2002) (g/kWh) | | – | 1.0 | 3.5 | 6.0 |
| | Normalized coefficients | 1 | 0.69 | 0.20 | 0.11 |
| Iteration 1 | Weighting factors | $\frac{1}{4} = 0.25$ | $\frac{1}{4} = 0.25$ | $\frac{1}{4} = 0.25$ | $\frac{1}{4} = 0.25$ |
| | Obtained values (g/kWh) | 246.21 | 0.88 | 1.34 | 37.72 |
| Iteration 2 | Weighting factors | $\frac{1}{9} = 0.11$ | $\frac{1}{9} = 0.11$ | $\frac{1}{9} = 0.11$ | $\frac{6}{9} = 0.67$ |
| | Obtained values (g/kWh) | 251.38 | 0.62 | 1.23 | 28.36 |
| Iteration 3 | Weighting factors | $\frac{1}{33} = 0.03$ | $\frac{1}{33} = 0.03$ | $\frac{1}{33} = 0.03$ | $\frac{30}{33} = 0.91$ |
| | Obtained values (g/kWh) | 264.57 | 0.66 | 2.44 | 15.04 |
| Iteration 4 | Weighting factors | $\frac{1}{93} = 0.01$ | $\frac{1}{93} = 0.01$ | $\frac{1}{93} = 0.01$ | $\frac{90}{93} = 0.97$ |
| | Obtained values (g/kWh) | 264.57 | 0.66 | 2.44 | 15.04 |

**Table 4**
Minimized fuel consumption and emissions optimization parameters.

| | |
|---|---|
| **Cost function** | Minimized fuel consumption and emissions |
| **Design variables** | $n_e$: engine speed<br>*gn*: transmission gear number<br>*th*: throttle position |
| **Variable bounds** | 700 rpm $\leq n_e \leq$ 2400 rpm<br>$1 \leq gn \leq 3$<br>$0\% \leq th \leq 100\%$ |

**Table 5**
Solutions of the proposed optimization problem.

| Digging depth (m) | Fuel rate (g/kWh) | *HC* (g/kWh) | *CO*(g/kWh) | *NOx* (g/kWh) |
|---|---|---|---|---|
| 0.1 | 326 | 2.09 | 0.00 | 36.60 |
| 0.2 | 295 | 1.10 | 2.07 | 23.83 |
| 0.3 | 265 | 0.66 | 2.44 | 15.04 |
| 0.4 | 243 | 0.46 | 1.62 | 9.84 |
| 0.5 | 225 | 0.31 | 0.80 | 9.33 |
| 0.6 | 212 | 0.26 | 0.89 | 8.15 |

concerning the digging depth is shown in Fig. 7. As it is shown, the objective function decreases as the digging depth increases, since the engine is working at higher efficiency points.

It is worth noting that the objective function resembles the overall pollution and consumption altogether, with the use of respective weighting factor for each item. This value is obtained after selecting the optimum working point of the engine, which can lead to the accomplishment of the functional goal defined for the bulldozer. Therefore, this graph shows an actual decrease in overall emissions (consisting of the three items of *HC*, *CO*, *NOx*) and fuel consumption, despite one item (in this case *CO*) may increase at each of the states. The improvement of emissions and fuel consumption with depth is due to the general trend of the engine toward the most efficient working zones, which are visible in each of the contours of Fig. 1. Moreover, the theoretical digging depth which minimizes the objective function would be observable based on the engine map contours. To reduce the number of figures, variations of the consumption and emission items are presented in Table 5, and the values of the overall objective function are plotted in Fig. 7.

The obtained design variables, i.e., engine control variables, for the proposed optimization problem are listed in Table 6. The results show that:

- The optimal range of engine speed is between 1800 and 2400 rpm.
- The third gear leads to the best fuel consumption and emissions, compared with other gear numbers.
- The throttle position increases as the demanded digging depth increases.

The obtained results for the design variables may be employed to develop an optimal control. It is worth mentioning that the actual speed of the machine can be calculated using Eq. (6). However, time and velocity are significant for construction vehicle performance optimization. In this paper, the performance is calculated for “energy” units (kWh), not based on the “power” units (kW). This approach inherently directs the problem to find the optimum solution in the vehicle's highest possible (optimum) speed range. However, imposing a strict exact time restriction or a minimum speed limitation would probably force the engine out of the current optimum working point, toward a sub-optimal point satisfying the time or speed constraints. This adversely affects the optimization results in terms of air pollution and fuel consumption, although providing an acceptable amount of improvement compared with the conditions of operation in non-optimal engine working points.

### 4.2. Terrain type effect

Finally, to illustrate the effectiveness of the proposed method for different terrain types, the digging programs are investigated for two new terrains; clayey soil and snow, the specifications of which are listed in Table 7.

The drawbar pull-slip curve for the dry sand is shown in Fig. 8. Table 8 shows the results of the optimum digging program for clayey soil. For each digging depth target, two rows are presented in this table; one row shows the performance of the bulldozer when using the operating conditions obtained during the optimization process for dry sand terrain and another row when using the working conditions obtained after performing re-optimization considering the clayey soil

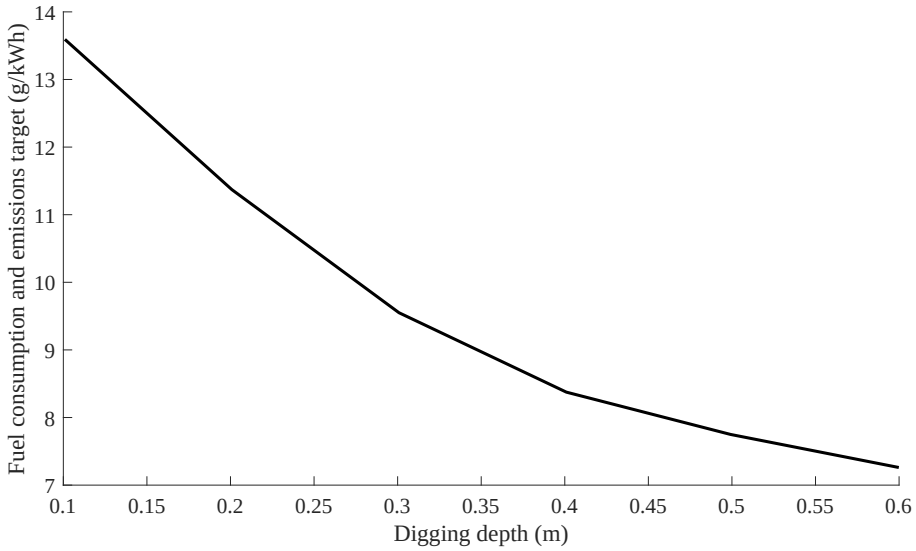


**Fig. 7.** Fuel consumption and emissions concerning the digging depth (Eq. (9)).

**Table 6**
Solutions of the engine control variables for the proposed optimization problem.

| Digging depth (m) | Engine speed $n_e$ (rpm) | Transmission gear number | Throttle position *gn th* (%) |
|---|---|---|---|
| 0.1 | 2372 | 3 | 18 |
| 0.2 | 2385 | 3 | 26 |
| 0.3 | 2374 | 3 | 37 |
| 0.4 | 2385 | 3 | 52 |
| 0.5 | 2120 | 3 | 60 |
| 0.6 | 1860 | 3 | 73 |

**Table 7**
Clayey soil and snow terrain specifications [14, 46].

| Parameter | Unit | Clayey soil | Snow |
|---|---|---|---|
| $n$ | – | 0.5 | 0.6 |
| $\phi$ | (Degrees) | 13.0 | 19.7 |
| $c$ | (kPa) | 4.14 | 1.03 |
| $k_\phi$ | (kN/m$^{n+2}$) | 692 | 197 |
| $k_c$ | (kN/m$^{n+1}$) | 13.19 | 4.37 |

conditions. The results show that the errors of the demanded and the actual digging depths for the cases where working conditions are optimized for the previous terrain type (dry sand) and the new soil (clayey soil) are up to 15%. This outcome shows the necessity of resolving the optimization problem for each terrain type. Besides, fuel consumption and emission targets are improved up to 6% for the re-optimized cases.

The drawbar pull-slip curve for snow is shown in Fig. 9. Table 9 shows the results of the optimum digging program for the snow terrain. The results show that the errors of the demanded and the actual digging depths are very high (100% in some cases) when the optimization problem is not resolved for the new soil type (snow). After resolving the digging problem considering the snow soil, not only fuel efficiency and emissions are improved, but also it facilitates the provision of the

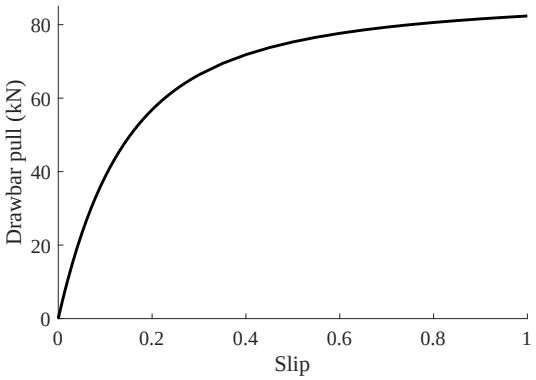


**Fig. 8.** Drawbar pull-slip curves for a tracked vehicle in clayey soil.

demanded digging depth. The results indicate that if the digging problem is not resolved for the new terrain type (and the optimum working parameters of dry sand are used for snow), the bulldozer could not reach the demanded digging depth in most cases. Besides, for the re-optimized cases, fuel efficiency and emissions targets are improved by up to 77%, which are more than the improvement values obtained for the clayey soil terrain.

## 5. Conclusion

A novel optimization model is developed for heavy tracked construction equipment which can be used for optimizing the vehicle performance in terms of fuel consumption and emissions (*HC*, *CO*, and *NOx*). The proposed model considers a complete range of engine operating points, taking into account fuel consumption and emission maps to accurately model the level of emission and fuel efficiency for different working conditions. For expanding the proposed approach to other construction vehicles, some modifications are needed. For example, the terramechanics equations for the tracked and wheeled vehicles are not the same. Moreover, the forces acting upon the blade are different for different machines. Therefore, for expanding this approach to other vehicle types, some changes should be applied. However, the core of the proposed method in this article is maintained without the need for major modifications. In this article, the productivity is ignored to concentrate on fuel consumption and emissions reduction, because of the simplicity. If more objective functions are augmented to the optimization problem, the solution method might even deviate from the

**Table 8**
Results of the optimum digging program for clayey soil.

| Demanded digging depth (m) | Optimization program conditions | Engine speed $n_e$ (rpm) | Gear number *gn* | Throttle position *th* | Actual digging depth (m) (error %) | Fuel & emissions target (g/kWh) (improv. %) |
|---|---|---|---|---|---|---|
| 0.10 | Opt. for dry sand | 2372 | 3 | 18 | 0.10 (0%) | 13.59 |
| | ReOpt. for clayey soil | 2337 | 3 | 18 | 0.10 | 13.56 (0%) |
| 0.20 | Opt. for dry sand | 2385 | 3 | 26 | 0.17 (15%) | 11.37 |
| | ReOpt. for clayey soil | 2355 | 3 | 29 | 0.20 | 10.70 (6%) |
| 0.30 | Opt. for dry sand | 2374 | 3 | 37 | 0.26 (13%) | 9.55 |
| | ReOpt. for clayey soil | 2366 | 3 | 42 | 0.30 | 9.02 (6%) |
| 0.40 | Opt. for dry sand | 2385 | 3 | 52 | 0.37 (8%) | 8.38 |
| | ReOpt. for clayey soil | 2292 | 3 | 54 | 0.40 | 8.13 (3%) |
| 0.50 | Opt. for dry sand | 2120 | 3 | 60 | 0.48 (4%) | 7.75 |
| | ReOpt. for clayey soil | 2124 | 3 | 64 | 0.50 | 7.64 (1%) |
| 0.60 | Opt. for dry sand | 1860 | 3 | 73 | 0.59 (2%) | 7.26 |
| | ReOpt. for clayey soil | 1769 | 3 | 73 | 0.60 | 7.28 (0%) |

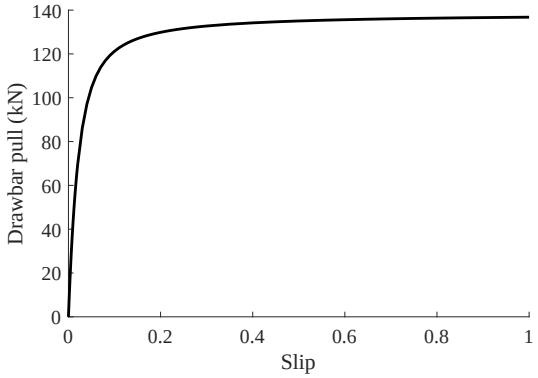


**Fig. 9.** Drawbar pull-slip curves for a tracked vehicle in snow.

primary goal. On the other hand, several studies are reported in the literature focusing on machine productivity; however, what is less discussed is an investigation of the fuel consumption and emissions at different machine working conditions, as an essential gap in the literature.

As a case study, a 40-ton tracked bulldozer on dry sandy soil is modeled. Fuel consumption and emission maps of the bulldozer engine are utilized. In the proposed optimization problem, a certain digging depth is specified, and minimum fuel consumption and emissions are targeted. In order to develop the corresponding combined optimization problem, normalization coefficients are obtained according to the EU non-road diesel engine standard targets, and weighting factors are assigned to each of the target items. An iterative process is proposed to find the proper weighting factors.

Results of the proposed problem show that:

- As the digging depth increases, the combined fuel consumption and emission target decreases, since the engine is operating at more efficient operating points.
- The proposed approach inherently directs the problem to find the optimum solution in the vehicle's highest possible (optimum) speed range, i.e., engine speeds are higher than 1700 rpm and the optimum gear numbers are 3.
- Imposing a strict exact time restriction or a minimum speed limitation would probably force the engine out of the current optimum working point, toward a sub-optimal point satisfying the time or speed constraints.
- The throttle position increases as the demanded digging depth increases.

In order to illustrate the effectiveness of the proposed method for different terrain types, the digging programs are investigated for two new terrains; clayey soil and snow. The results show that the optimization problem should be carried out distinctly for each terrain type for two reasons: satisfying the digging demand and optimizing fuel efficiency and emissions targets. The presented results indicate that this leads to an improvement of up to 77% in fuel efficiency and emissions targets. On the other hand, without repeating the optimization considering the terrain specifications, the error of the digging depth may increase to relatively high values, and the bulldozer may not even be able to reach the specified digging depth using the pre-specified engine operating point.

The bulldozer digging optimization model presented in this paper may be used for steady-state maneuvers as well. Also, the results may be stored in look-up tables to be employed for dynamic and optimal control problems in real-time. If the terrain specifications are unknown, an identification algorithm can be used to develop an on-line optimization problem, concerning the terrain specifications.

The proposed methodology can be used for fuel consumption

**Table 9**
Results of the optimum digging program for snow.

| Demanded digging depth (m) | Optimization program conditions | Engine speed $n_e$ (rpm) | Gear number *gn* | Throttle position *th* | Actual digging depth (m) (error %) | Fuel & emissions target (g/kWh) (improv. %) |
|---|---|---|---|---|---|---|
| 0.10 | Opt. for dry sand | 2372 | 3 | 18 | 0.00 (100%) | 13.59 |
| | ReOpt. for snow | 2120 | 3 | 63 | 0.10 | 7.66 (77%) |
| 0.20 | Opt. for dry sand | 2385 | 3 | 26 | 0.00 (100%) | 11.37 |
| | ReOpt. for snow | 2113 | 3 | 68 | 0.20 | 7.54 (51%) |
| 0.30 | Opt. for dry sand | 2374 | 3 | 37 | 0.00 (100%) | 9.55 |
| | ReOpt. for snow | 1971 | 3 | 72 | 0.31 | 7.35 (30%) |
| 0.40 | Opt. for dry sand | 2385 | 3 | 52 | 0.00 (100%) | 8.38 |
| | ReOpt. for snow | 2389 | 3 | 99 | 0.40 | 7.39 (13%) |
| 0.50 | Opt. for dry sand | 2120 | 3 | 60 | 0.00 (100%) | 7.75 |
| | ReOpt. for snow | 2159 | 3 | 98 | 0.50 | 7.13 (9%) |
| 0.60 | Opt. for dry sand | 1860 | 3 | 73 | 0.34 (43%) | 7.26 |
| | ReOpt. for snow | 1736 | 3 | 100 | 0.60 | 6.93 (5%) |

optimization and emissions reduction in other commercial and off-road vehicles, chiefly agricultural and construction vehicles, the performances of which are governed by their interaction with the terrain. In this paper, a case study of tracked bulldozer is considered. However, the same methodology can be applied to pneumatic-tire heavy construction vehicles.

## Declaration of Competing Interest

The authors declare that they have no known competing financial interests or personal relationships that could have appeared to influence the work reported in this paper.

## References


[1] J. Yamaura, S.T. Muench, Assessing the impacts of mobile technology on public transportation project inspection, Autom. Constr. 96 (2018) 55–64, https://doi.org/10.1016/j.autcon.2018.08.021.

[2] M. Ziyadi, H. Ozer, S. Kang, I.L. Al-Qadi, Vehicle energy consumption and an environmental impact calculation model for the transportation infrastructure systems, J. Clean Prod. 174 (2018) 424–436, https://doi.org/10.1016/j.jclepro.2017.10.292.

[3] X. Tao, C. Mao, F. Xie, G. Liu, P. Xu, Greenhouse gas emission monitoring system for manufacturing prefabricated components, Autom. Constr. 93 (2018) 361–374, https://doi.org/10.1016/j.autcon.2018.05.015.

[4] R.S. Nizam, C. Zhang, L. Tian, A BIM based tool for assessing embodied energy for buildings, Energy and Buildings 170 (2018) 1–14, https://doi.org/10.1016/j.enbuild.2018.03.067.

[5] M.L. Trani, B. Bossi, M. Gangolells, M. Casals, Predicting fuel energy consumption during earthworks, J. Clean Prod. 112 (2016) 3798–3809, https://doi.org/10.1016/j.jclepro.2015.08.027.

[6] M. Sandanayake, G. Zhang, S. Setunge, C.-Q. Li, J. Fang, Models and method for estimation and comparison of direct emissions in building construction in Australia and a case study, Energy Build. 126 (2016) 128–138, https://doi.org/10.1016/j.enbuild.2016.05.007.

[7] P.O. Akadiri, P.O. Olomolaiye, E.A. Chinyio, Multi-criteria evaluation model for the selection of sustainable materials for building projects, Autom. Constr. 30 (2013) 113–125, https://doi.org/10.1016/j.autcon.2012.10.004.

[8] B. Muresan, A. Capony, M. Goriaux, D. Pillot, P. Higelin, C. Proust, A. Jullien, Key factors controlling the real exhaust emissions from earthwork machines, Transp. Res. D Transp. and Environ. 41 (2015) 271–287, https://doi.org/10.1016/j.trd.2015.10.002.

[9] M. Sandanayake, G. Zhang, S. Setunge, W. Luo, C.-Q. Li, Estimation and comparison of environmental emissions and impacts at foundation and structure construction stages of a building — a case study, J. Clean Prod. 151 (2017) 319–329, https://doi.org/10.1016/j.jclepro.2017.03.041.

[10] T. Chen, W. Zhuge, Y. Zhang, L. Zhang, A novel cascade organic Rankine cycle (ORC) system for waste heat recovery of truck diesel engines, Energy Convers. Manag. 138 (2017) 210–223, https://doi.org/10.1016/j.enconman.2017.01.056.

[11] H. Kua, Integrated policies to promote sustainable use of steel slag for construction — a consequential life cycle embodied energy and greenhouse gas emission perspective, Energy Build. 101 (2015) 133–143, https://doi.org/10.1016/j.enbuild.2015.04.036.

[12] H. Tajeen, Z. Zhu, Image dataset development for measuring construction equipment recognition performance, Autom. Constr. 48 (2014) 1–10, https://doi.org/10.1016/j.autcon.2014.07.006.

[13] I. Flood, P. Christophilos, Modeling construction processes using artificial neural networks, Autom. Constr. 4 (4) (1996) 307–320, https://doi.org/10.1016/0926-5805(95)00011-9.

[14] M.G. Bekker, Off-the-road locomotion, ISBN: 978-04-720-4142-8 Michigan University Press, 1960.

[15] S. Taheri, C. Sandu, S. Taheri, E. Pinto, D. Gorsich, A technical survey on Terramechanics models for tire–terrain interaction used in modeling and simulation of wheeled vehicles, J. Terrramech. 57 (2015) 1–22, https://doi.org/10.1016/j.jterra.2014.08.003.

[16] A. Sane, T.M. Wasfy, H.M. Wasfy, J.M. Peters, Coupled multibody dynamics and discrete element modeling of bulldozers cohesive soil moving operation, 11th International Conference on Multibody Systems, Nonlinear Dynamics, and Control, vol. 6, ASME, 2015, , https://doi.org/10.1115/detc2015-47133.

[17] A.G. Sane, High-fidelity modelling of a bulldozer using an explicit multibody dynamics finite element code with integrated discrete element method, Ph.D. thesis https://scholarworks.iupui.edu/handle/1805/6441, (2015) Date of last access: 3-19-2019.

[18] M.G. Bekker, Introduction to Terrain-Vehicle Systems, ISBN: 978-04-720-4144-2 University of Michigan Press, 1969.

[19] B.D. Zhang, X. Zhang, L. Zhang, L.H. Xi, Development and validation of a series hybrid electric bulldozer model on whole working condition, Key Eng. Mater. 693 (2016) 1811–1817, https://doi.org/10.4028/www.scientific.net/kem.693.1811.

[20] M. Pan, J. Yan, Q. Tu, C. Jiang, Research on the multi-energy management strategy of the electric drive system of a tracked bulldozer, Math. Probl. Eng. 2016 (2016) 1–13, https://doi.org/10.1155/2016/5631209.

[21] H. Wang, Y. Huang, A. Khajepour, Q. Song, Model predictive control-based energy management strategy for a series hybrid electric tracked vehicle, Appl. Energy 182 (2016) 105–114, https://doi.org/10.1016/j.apenergy.2016.08.085.

[22] P. Lewis, A. Hajji, Comparison of two models for estimating equipment productivity for a sustainability quantification tool, ICSDEC 2012, American Society of Civil Engineers, 2012, , https://doi.org/10.1061/9780784412688.075.

[23] P. Lewis, A. Hajji, Estimating the economic, energy, and environmental impact of earthwork activities, Construction Research Congress 2012, American Society of Civil Engineers, 2012, , https://doi.org/10.1061/9780784412329.178.

[24] A. Hajji, The use of construction equipment productivity rate model for estimating fuel use and carbon dioxide ($CO_2$) emissions case study: bulldozer, excavator and dump truck, Int. J. Sustain. Eng. 8 (2) (2014) 111–121, https://doi.org/10.1080/19397038.2014.962645.

[25] C. Ahn, W. Pan, S. Lee, F. Peña-Mora, Enhanced estimation of air emissions from construction operations based on discrete-event simulation, Proceedings of the International Conference on Computing in Civil and Building Engineering (ICCCBE) Nottingham, UK, vol. 30, 2010, pp. 237–243 ISBN:978-1-907284-60-1.

[26] K. Barati, X. Shen, Operational level emissions modelling of on-road construction equipment through field data analysis, Autom. Constr. 72 (2016) 338–346, https://doi.org/10.1016/j.autcon.2016.08.010.

[27] EPA, User's Guide for the Final NONROAD 2005 Model, EPA-420-R-05-013, United States Environmental Protection Agency, Office of Transportation and Air Quality, 2005, Date of last access: 3-19-2019, https://nepis.epa.gov/Exe/ZyPURL.cgi?Dockey=P1004L24.TXT.

[28] J.D. Robinson, F. Vahedifard, M. Rais-Rohani, G.L. Mason, J.D. Priddy, Multi-objective traction optimization of vehicles in loose dry sand using the generalized reduced gradient method, J. Terrramech. 64 (2016) 46–57, https://doi.org/10.1016/j.jterra.2015.12.005.

[29] F. Vahedifard, J.D. Robinson, G.L. Mason, I.L. Howard, J.D. Priddy, Mobility algorithm evaluation using a consolidated database developed for wheeled vehicles operating on dry sands, J. Terrramech. 63 (2016) 13–22, https://doi.org/10.1016/j.jterra.2015.10.002.

[30] A.K. Richmond, R.K. Kaufmann, Is there a turning point in the relationship between income and energy use and/or carbon emissions? Ecol. Econ. 56 (2) (2006) 176–189, https://doi.org/10.1016/j.ecolecon.2005.01.011.

[31] M.R. Lotfalipour, M.A. Falahi, M. Ashena, Economic growth, $CO_2$ emissions, and fossil fuels consumption in Iran, Energy 35 (12) (2010) 5115–5120, https://doi.org/10.1016/j.energy.2010.08.004.

[32] I. Hanif, S.M.F. Raza, P. Gago-de Santos, Q. Abbas, Fossil fuels, foreign direct investment, and economic growth have triggered $CO_2$ emissions in emerging Asian economies: some empirical evidence, Energy 171 (2019) 493–501, https://doi.org/10.1016/j.energy.2019.01.011.

[33] Y. Xiao, A. Konak, A genetic algorithm with exact dynamic programming for the green vehicle routing & scheduling problem, J. Clean Prod. 167 (2017) 1450–1463, https://doi.org/10.1016/j.jclepro.2016.11.115.

[34] M. Masih-Tehrani, S. Ebrahimi-Nejad, Hybrid genetic algorithm and linear programming for bulldozer emissions and fuel-consumption management using continuously variable transmission, J. Constr. Eng. Manag. 144 (7) (2018) 04018053, https://doi.org/10.1061/(asce)co.1943-7862.0001490.

[35] P. Lewis, W. Rasdorf, H.C. Frey, S.-H. Pang, K. Kim, Requirements and incentives for reducing construction vehicle emissions and comparison of nonroad diesel engine emissions data sources, Journal of Construction Engineering and Management 135 (5) (2009) 341–351, https://doi.org/10.1061/(asce)co.1943-7862.0000008.

[36] Caterpillar, Caterpillar Performance Handbook, ISBN: 978-00-000-2648-4 Caterpillar Incorporated, 2018.

[37] T. Markel, A. Brooker, T. Hendricks, V. Johnson, K. Kelly, B. Kramer, M. OKeefe, S. Sprik, K. Wipke, ADVISOR: a systems analysis tool for advanced vehicle modeling, J. Power Sources 110 (2) (2002) 255–266, https://doi.org/10.1016/S0378-7753(02)00189-1.

[38] Z. Qin, Y. Luo, K. Li, H. Peng, Optimal design of single-mode power-split hybrid tracked vehicles, J. Dyn. Syst. Meas. Control 140 (10) (2018) 101002, https://doi.org/10.1115/1.4039687.

[39] S. Borthakur, S.C. Subramanian, Design and optimization of a modified series hybrid electric vehicle powertrain, Proc. IME D J. Automob. Eng. (2018), https://doi.org/10.1177/0954407018759357 095440701875935.

[40] P. Dekraker, D. Barba, A. Moskalik, K. Butters, Constructing engine maps for full vehicle simulation modeling, Tech. rep. SAE Technical Paper, 2018, , https://doi.org/10.4271/2018-01-1412.

[41] Q. Zhao, Q. Chen, L. Wang, Real-time prediction of fuel consumption based on digital map API, Appl. Sci. 9 (7) (2019) 1369, https://doi.org/10.3390/app9071369.

[42] E. Wood, J. Gonder, F. Jehlik, On-road validation of a simplified model for estimating real-world fuel economy, SAE Int. J. Fuels and Lubr. 10 (2) (2017) 528–536, https://doi.org/10.4271/2017-01-0892.

[43] K. Barati, X. Shen, Optimal driving pattern of on-road construction equipment for emissions reduction, Procedia Eng. 180 (2017) 1221–1228, https://doi.org/10.1016/j.proeng.2017.04.283.

[44] J.Y. Wong, Theory of Ground Vehicles, ISBN: 978-04-701-7038-0 John Wiley & Sons, 2008.

[45] J.Y. Wong, Terramechanics and off-road vehicle engineering: terrain behaviour, off-road vehicle performance and design, ISBN: 978-07-506-8561-0 Elsevier, 2010.

[46] G. Mastinu, M. Ploechl, Road and Off-Road Vehicle System Dynamics Handbook, ISBN: 978-11-380-7529-0 CRC Press, 2014.

[47] W.-S. Lee, J.-H. Kim, J.-H. Cho, A driving simulator as a virtual reality tool, Proceedings. 1998 IEEE International Conference on Robotics and Automation (Cat. No. 98CH36146), 1 IEEE, 1998, pp. 71–76, , https://doi.org/10.1109/robot.1998.676264.

[48] B. Mashadi, D. Crolla, Vehicle Powertrain Systems, ISBN: 978-04-706-6602-9 John Wiley & Sons, Ltd., 2012, https://doi.org/10.1002/9781119958376.

[49] C.R. Houck, J. Joines, M.G. Kay, A genetic algorithm for function optimization: a Matlab implementation, NCSU-IE TR 95 (09) (1995), http://www.igi.tugraz.at/lehre/MLB/WS12/task1.zip.

[50] T. Yokota, M. Gen, Y. Li, C.E. Kim, A genetic algorithm for interval nonlinear integer programming problem, Comput. Ind. Eng. 31 (3-4) (1996) 913–917, https://doi.org/10.1016/s0360-8352(96)00263-x.

[51] DieselNet, EU: Nonroad Engines Emission Standard Date of last access: 3-19-2019, www.dieselnet.com/standards/eu/nonroad.php.

[52] A.A. Zardini, R. Suarez-Bertoa, F. Forni, F. Montigny, M. Otura-Garcia, M. Carriero, C. Astorga, Reducing the exhaust emissions of unregulated pollutants from small gasoline engines with alkylate fuel and low-ash lube oil, Environ. Res. 170 (2019) 203–214, https://doi.org/10.1016/j.envres.2018.12.021.

[53] D. Llopis-Castelló, F.J. Camacho-Torregrosa, A. García, Analysis of the influence of geometric design consistency on vehicle $CO_2$ emissions, Transp. Res. D Trans. Environ. 69 (2019) 40–50, https://doi.org/10.1016/j.trd.2019.01.029.

[54] A.R. Patil, A. Desai, Optimization of application of 2-ethyl-hexyl-nitrate on partial substitution of ethanol in CI engine for fuel economy and emission control using MADM method, SN Appl. Sci. 1 (2) (2019) 166, https://doi.org/10.1007/s42452-019-0163-7.

[55] C. Mazzoleni, H. Moosmüller, H.D. Kuhns, R.E. Keislar, P.W. Barber, D. Nikolic, N.J. Nussbaum, J.G. Watson, Correlation between automotive CO, HC, NO, and PM emission factors from on-road remote sensing: implications for inspection and maintenance programs, Transp. Res. D Trans. Environ. 9 (6) (2004) 477–496, https://doi.org/10.1016/j.trd.2004.08.006.